Oscillations of Cytosolic Sodium During Calcium Oscillations in Exocrine Acinar Cells

MONICA M. Y. WONG AND J. KEVIN FOSKETT*

In acinar cells from rat salivary glands, cholinergic agonists cause oscillations in cytoplasmic free calcium concentration, which then drive oscillations of cell volume that reflect oscillating cell solute content and fluid secretion. By quantitative fluorescence ratio microscopy of an intracellular indicator dye for sodium, it has now been shown that large amplitude oscillations of sodium concentration were associated with the calcium and cell volume oscillations. Both calcium and sodium oscillations were dependent on the continued presence of calcium in the extracellular medium and were abolished by the specific sodium-potassium adenosine triphosphatase inhibitor ouabain. Thus, calcium oscillations in salivary acinar cells, by modulating the activities of ion transport pathways in the plasma membrane, can cause significant oscillations of monovalent ions that may in turn feed back to regulate calcium oscillations and fluid secretion.

IN A WIDE VARIETY OF CELL TYPES, external signals induce oscillations in the concentration of cytoplasmic free calcium ($[Ca^{2+}]_i$) (*1*). A number of hypothetical schemes have been proposed to account for oscillations (*1*), but the mechanisms that underlie $[Ca^{2+}]_i$ oscillations in nonexcitable cells are not clear. Muscarinic cholinergic stimulation of acinar cells from the salivary glands (parotid) of rats induces $[Ca^{2+}]_i$ oscillations, which require continued receptor occupancy to be maintained (*2*). Identical oscillations can be induced in the absence of receptor stimulation or elevated inositol phosphate concentrations by exposure of these cells to thapsigargin (TG) (*3*) or cyclopiazonic acid (*4*), microsomal Ca^{2+} adenosine triphosphatase (ATPase) inhibitors. Because these $[Ca^{2+}]_i$ oscillations can be enhanced by caffeine and inhibited by ryanodine (*5*), they may be driven by periodic Ca^{2+} release from an inositol (1,4,5)-trisphosphate (IP_3)–insensitive Ca^{2+} store with properties similar to sarcoplasmic reticulum of excitable cells. These oscillations are sustained by Ca^{2+} influx across the plasma membrane, which is regulated by the amount of Ca^{2+} in the IP_3-sensitive store (*3, 5*).

The physiological consequences of oscillating $[Ca^{2+}]_i$ are unknown in any cell. Oscillations of $[Ca^{2+}]_i$ induced in parotid acinar cells by muscarinic stimulation or TG are associated with oscillations of cell volume (*2, 6*) (Fig. 1A). These $[Ca^{2+}]_i$-induced changes in cell volume are a direct reflection of simultaneous changes of cell solute content (7), suggesting that cell solute (Cl^- plus a cation) content oscillates during $[Ca^{2+}]_i$ oscillations. Thus, cell shrinkage induced by elevated $[Ca^{2+}]_i$ is the result of solute loss, whereas volume recovery that follows shrinkage is a result of net solute accumulation by the cell. These cell volume changes during $[Ca^{2+}]_i$ oscillations can be interpreted within the context of a model of fluid secretion from epithelial cells driven by Cl^- secretion (*5*). Thus, a rise of $[Ca^{2+}]_i$ activates K^+ channels in the basolateral membrane and Cl^- channels in the apical membrane, causing KCl (and therefore water) loss, which results in cell shrinkage. Return of $[Ca^{2+}]_i$ toward resting levels, either as a result of agonist removal or during $[Ca^{2+}]_i$ oscillations (*5*), reduces this KCl permeability, allowing ion influx mechanisms in the basolateral membrane to restore cell solute content. Alternating activation and inactivation of these solute efflux and influx pathways indicates that fluid secretion oscillates during $[Ca^{2+}]_i$ oscillations (*5*). The influx pathways likely include a Na^+-K^+-Cl^- cotransporter (*8, 9*), and parallel Na^+-H^+ and Cl^--HCO_3^- exchangers (*9, 10*). The energy for these salt uptake pathways is derived from the Na^+ gradient between the cytoplasm and extracellular medium, which is maintained by the Na^+,K^+-ATPase in the basolateral membrane.

Because of the importance of Na^+ in the mechanisms underlying Cl^- and fluid secretion in salivary acinar cells and other secretory epithelial cells, we measured the intracellular Na^+ concentration ($[Na^+]_i$) in single parotid acinar cells during $[Ca^{2+}]_i$ oscillations by ratio imaging of a fluorescent indicator dye for Na^+ [benzofuran phthalate (SBFI)] (*11*). Under control conditions, resting $[Na^+]_i$ in these cells was 9.4 ± 0.7 mM (*12*) (mean ± SE; n = 55 cells on 11 cover slips, obtained from six rats).

We determined $[Na^+]_i$ during $[Ca^{2+}]_i$ oscillations by simultaneous fluorescence determinations of $[Na^+]_i$ and differential interference contrast imaging of cell volume in SBFI-loaded cells (Fig. 1B). Exposure of the cell in Fig. 1B to TG plus caffeine (*6*) caused the cell volume to oscillate, reflecting oscillating $[Ca^{2+}]_i$. Examination of SBFI fluorescence ratios simultaneously determined in the same cell reveals that these volume, that is, $[Ca^{2+}]_i$, changes were associated with

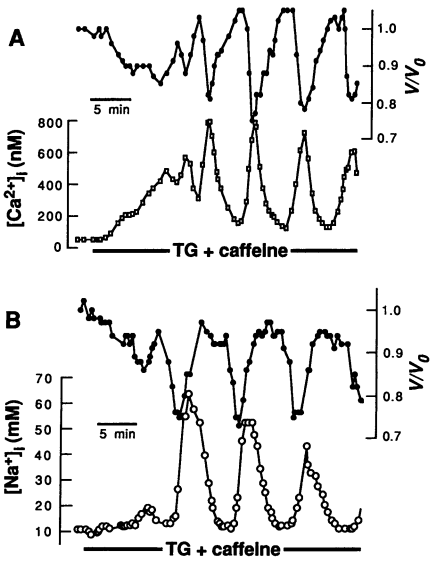

Fig. 1. Intracellular Ca^{2+} concentration (**A**) (□) and intracellular Na^+ concentration (**B**) (○) and cell volume (●) in single parotid acinar cells during exposure to TG (2 μM) plus caffeine (10 mM). The curves are the results from single cells chosen to be representative of 25 (A) and 55 cells (B). Single parotid acinar cells from male Wistar rats were obtained by sequential trypsin and collagenase digestion (*3, 5*). Experiments were conducted in a saline consisting of (in mM): 135 mM Na^+, 115.4 mM Cl^-, 5.4 mM K^+, 25 mM HCO_3^-, 0.73 mM PO_4^{2-}, 0.8 mM SO_4^{2-}, 0.8 mM Mg^{2+}, 20 mM Hepes, 2 mM glutamine, 10 mM glucose, pH 7.4, with 95% O_2 and 5% CO_2 at 37°C. Cells adhering to polylysine-coated cover slips were loaded with the fluorescent indicator dyes and used within 10 to 60 min of loading. The cover slip was perfused continuously at 2 ml/min (bath volume, 50 μl) with standard HCO_3^- medium at 37°C on the stage of an inverted microscope (Zeiss IM35). All data were obtained from single cells existing as individuals or within doublets or "strings" of cells consisting of up to five cells. The Ca^{2+} indicator dye fura-2 was used as described (*2, 3, 5*). For $[Na^+]_i$ determinations, cells were loaded with SBFI by incubation with 7 μM SBFI–acetoxymethyl ester (dissolved in a 1:1 mixture of dimethyl sulfoxide and 25% pluronic acid) for 60 min at room temperature or 37°C. The SBFI fluorescence excitation and emission collection, construction of ratio images, and quantitation (*12*) were as described for fura-2 (*2, 3, 5*). During $[Ca^{2+}]_i$ or $[Na^+]_i$ determinations, cells were viewed in differential interference contrast (DIC) and fluorescence optics with a ×63 oil, 1.25 numerical aperture objective lens. The microscope is designed to allow simultaneous DIC imaging and low-light fluorescence measurements without the light losses normally associated with DIC (*18*). A video disk recorder that interfaced to a second video detector recorded the DIC image of the same cell synchronously with the digitization of the fluorescence image. An estimate of cell volume was obtained by planimetry of the DIC images (*2, 7*). Cell volume (V) was normalized to the initial cell volume determined under resting conditions (V_0).

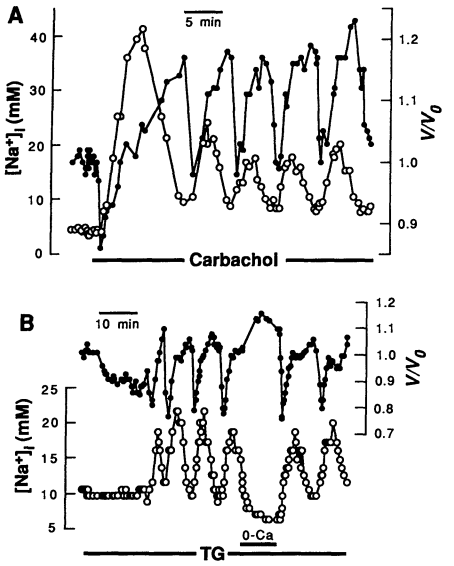

Fig. 2. $[Na^+]_i$ (○) and cell volume (V/V_0) (●) oscillations in single parotid acinar cells during $[Ca^{2+}]_i$ oscillations induced by (**A**) carbachol (10 μM) or (**B**) TG (2 μM). Where indicated in (B) (0-Ca), extracellular Ca^{2+} (3 mM) was replaced with 1 mM EGTA. The curves are the results from single cells chosen to be representative of three (A) and five cells (B).

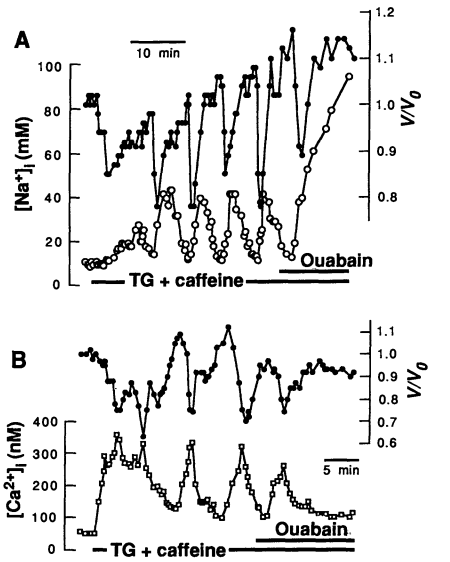

Fig. 3. Inhibition of $[Na^+]_i$ (**A**) (○) or $[Ca^{2+}]_i$ (**B**) (□) and cell volume (V/V_0) (●) oscillations by inhibition of the Na^+ pump with ouabain (1 mM). Oscillations were induced by TG (2 μM) plus caffeine (10 mM). The curves are the results from single cells chosen to be representative of 21 (A) and 24 cells (B).

substantial changes in $[Na^+]_i$. Resting $[Na^+]_i$ in this cell was ~10 mM. There was a gradual rise of $[Na^+]_i$ during the initial cell shrinkage when $[Ca^{2+}]_i$ was likely slowly rising. A transient elevation of $[Na^+]_i$ to ~20 mM was associated with the first, small $[Ca^{2+}]_i$ transient increase. Subsequently, the more vigorous $[Ca^{2+}]_i$ oscillations were associated with large $[Na^+]_i$ oscillations. The $[Na^+]_i$ oscillations lagged behind the volume oscillations, which slightly lagged behind the $[Ca^{2+}]_i$ oscillations (Fig. 1).

During each cycle, $[Na^+]_i$ first began to rise when the cell had reached maximal shrinkage, that is (from Fig. 1A), ~30 s after the peak $[Ca^{2+}]_i$ (*13*). The $[Na^+]_i$ rose to ~65 mM during the next 1 to 2 min (for 55 cells, peak $[Na^+]_i$ during oscillations was 49 ± 4 mM) (*14*). This rise to a peak was completed at a time when cell volume recovery was only ~50% complete. During the initial phase of the decline in $[Na^+]_i$, cell volume continued to increase. Subsequently, after cell volume had increased and then stabilized before the next cycle, $[Na^+]_i$ continued to fall to resting values in the cell in Fig. 1B and to 16 ± 1 mM in 55 cells. The lack of correspondence between $[Na^+]_i$ and cell volume during the falling phase of $[Na^+]_i$ indicates that Na^+ efflux was associated with influx of another cation, probably K^+. Similar $[Na^+]_i$ oscillations were associated with TG-induced $[Ca^{2+}]_i$ oscillations in all cells examined (n = 55). We verified that carbachol (10 μM) elicits $[Na^+]_i$ oscillations that are indistinguishable from those elicited by TG (Fig. 2A) (n = 3 cells).

The correlation between cell volume and $[Na^+]_i$ during volume oscillations suggested $[Na^+]_i$ oscillations are driven by $[Ca^{2+}]_i$ oscillations. The TG-induced $[Ca^{2+}]_i$ oscillations (*15*) as well as the $[Na^+]_i$ and cell volume oscillations were strictly dependent on the continuous presence of extracellular Ca^{2+} (Fig. 2B). These data, together with the temporal relations between changes in $[Ca^{2+}]_i$, cell volume, and $[Na^+]_i$, demonstrate that $[Na^+]_i$ oscillations are a result of oscillating $[Ca^{2+}]_i$.

The $[Na^+]_i$ in unstimulated parotid cells is similar to that believed to exist in most cells. Because $[Na^+]_i$ is thought to be tightly regulated by the ubiquitous Na^+,K^+-ATPase, we were surprised to observe such large excursions during $[Ca^{2+}]_i$ oscillations. The presence of $[Na^+]_i$ oscillations suggests the relative activities of Na^+ influx and efflux mechanisms must oscillate during $[Ca^{2+}]_i$ oscillations. To determine whether the Na^+,K^+-ATPase, the major Na^+ efflux pathway in cells, was involved in the falling phase of $[Na^+]_i$ during $[Na^+]_i$ oscillations, we exposed oscillating cells to ouabain, a specific inhibitor of the Na^+ pump. Addition of ouabain immediately before the next cycle in oscillating cells was without effect on the subsequent cell shrinkage, demonstrating that ouabain is without effect on the K^+ and Cl^- efflux pathways, or on the subsequent, normal rate of rise of $[Na^+]_i$, indicating lack of effect on the Na^+ influx pathways (Fig. 3A) (n = 24 cells on four cover slips, obtained from three animals). However, $[Na^+]_i$ continued to rise to values that were higher than those achieved during oscillations (*14*) and $[Na^+]_i$ oscillations, as well as cell volume oscillations were abolished. These data indicate that the falling phase of $[Na^+]_i$ during oscillations is mediated by the Na^+,K^+-ATPase. Dimethylamiloride (to block Na^+-H^+ exchange) together with bumetanide (to block Na^+-K^+-Cl^- cotransport) had no effect on the normal cell shrinkage associated with the rising phase of $[Ca^{2+}]_i$ but prevented the normal subsequent rise of $[Na^+]_i$ (*15*), indicating that the rising phase of $[Na^+]_i$ during oscillations is mediated by these Na^+ transport mechanisms.

The $[Ca^{2+}]_i$ spikes in each oscillating cell (n = 55) did not proceed until $[Na^+]_i$ returned to a value that was within a factor of 2 of the resting $[Na^+]_i$ in that cell (Figs. 1, 2, 3A), indicating that elevated $[Na^+]_i$ blocks the next $[Ca^{2+}]_i$ oscillation. Further, not only did ouabain stop both $[Na^+]_i$ and volume oscillations as well as raise $[Na^+]_i$ (Fig. 3A), but it also stopped the $[Ca^{2+}]_i$ oscillations (Fig. 3B) (n = 21 out of 21 cells).

We have demonstrated that induction of $[Ca^{2+}]_i$ oscillations in salivary acinar cells drives large amplitude $[Na^+]_i$ oscillations that result from Na^+ influx (Na^+-H^+ exchange and Na^+-K^+-Cl^- cotransport) and efflux (Na^+,K^+-ATPase) pathways in the basolateral membrane whose relative activities oscillate with a phase delay compared to the $[Ca^{2+}]_i$ oscillations. The influx rate of Na^+ exceeds the Na^+-pump–mediated efflux rate during the rising phase of $[Na^+]_i$, most likely due to activation of the influx pathways, by the rise of $[Ca^{2+}]_i$ or the consequent cell shrinkage or decrease in $[Cl^-]_i$ (*2, 7*). During the falling phase of $[Na^+]_i$, the pump-mediated Na^+ efflux rate exceeds the influx rate. This is likely in part a result of inactivation of the influx pathways, as the purported activating mechanisms (elevated $[Ca^{2+}]_i$, reduced cell volume, and $[Cl^-]_i$) are all returning to resting concentrations when $[Na^+]_i$ begins to decrease. Furthermore, the Na^+ gradient between the extracellular medium and cytoplasm is reduced. The similar rates of rise of $[Na^+]_i$ in the absence and presence of ouabain (Fig. 3A) imply that the pump is inactive during the rising phase of $[Na^+]_i$, suggesting that the falling phase of $[Na^+]_i$ is also a result of enhanced Na^+ efflux caused by delayed activation of the Na^+ pump.

Because cell volume reflects the Cl^- content of the cell, and therefore $[Cl^-]_i$ (*7*), cell volume oscillations imply that $[Cl^-]_i$ oscillates during $[Ca^{2+}]_i$ oscillations. Furthermore, the $[Na^+]_i$ oscillations are associated with $[K^+]_i$ oscillations (*16*). Thus, $[Ca^{2+}]_i$

oscillations in parotid acinar cells drive oscillations of secretion, $[Cl^-]_i$, $[Na^+]_i$, $[K^+]_i$, and cell volume. The temporal relations and $[Ca^{2+}]_i$ dependencies demonstrate that $[Ca^{2+}]_i$ is the primary signaling mechanism for these oscillations. Nevertheless, an issue to consider is whether oscillating concentrations of intracellular ions or water content are themselves regulatory signals. Our results suggest intracellular cation composition, modulated by $[Ca^{2+}]_i$ oscillations, may in turn modulate $[Ca^{2+}]_i$ oscillations. Oscillating concentrations of monovalent ions may cause the activities of transporters for which they are substrates to oscillate as well. For energy-dependent pumps (for example, the Na^+,K^+-ATPase), oscillations in their activities may result in oscillations of $[ATP]_i$ and cellular metabolism (*17*), which then may affect many cellular processes.

REFERENCES AND NOTES

1. M. J. Berridge, *J. Biol. Chem.* **265**, 9583 (1990); R. Jacob, *Biochim. Biophys. Acta* **1052**, 427 (1990).
2. J. K. Foskett and J. E. Melvin, *Science* **244**, 1582 (1989).
3. J. K. Foskett, C. Roifman, D. Wong, *J. Biol. Chem.* **266**, 2778 (1991).
4. J. K. Foskett and D. Wong, *Am. J. Physiol.*, in press.
5. ———, *J. Biol. Chem.* **266**, 14535 (1991).
6. Exposure of single parotid acinar cells to 2 μM TG plus 10 mM caffeine is the most reliable method to induce $[Ca^{2+}]_i$ oscillations (*5*). These oscillations are indistinguishable from those induced by TG alone.
7. J. K. Foskett, *Am. J. Physiol.* **259**, C998 (1990).
8. K. R. Lau, J. W. Howorth, R. M. Case, *J. Physiol. (London)* **425**, 407 (1990); R. J. Turner, J. N. George, B. J. Baum, *J. Membr. Biol.* **94**, 143 (1986); J. H. Poulsen and B. Nauntofte, *J. Dent. Res.* **66**, 608 (1987); R. Case, M. Hunter, I. Novak, J. A. Young, *J. Physiol. (London)* **349**, 619 (1984); L. H. Smaje, J. H. Poulsen, H. H. Ussing, *Pfluegers Arch.* **406**, 492 (1986).
9. S. P. Soltoff, M. K. McMillian, L. C. Cantley, E. J. Cragoe, Jr., B. R. Talamo, *J. Gen. Physiol.* **93**, 285 (1989); D. Pirani, A. R. Evans, D. I. Cook, J. A. Young, *Pfluegers Arch.* **408**, 178 (1987); S. Dissing and B. Nauntofte, *Am. J. Physiol.* **259**, G1044 (1990).
10. J. E. Melvin, A. Moran, R. J. Turner, *J. Biol. Chem.* **263**, 19564 (1988); M. Manganel and R. J. Turner, *ibid.* **265**, 4284 (1990); *J. Membr. Biol.* **111**, 191 (1989); J. R. Martinez, S. Barker, J. Camden, *Eur. J. Pharmacol.* **164**, 335 (1989); M. C. Steward, Y. Seo, R. M. Case, *Pfluegers Arch.* **414**, 200 (1989); I. Novak and J. A. Young, *ibid.*, p. 68.
11. A. Minta and R. Y. Tsien, *J. Biol. Chem.* **264**, 19449 (1989).
12. Intracellular SBFI fluorescence was diffusely distributed and concentrated in vesicular compartments. Extent of dye compartmentation was variable among cells and was more pronounced when loading was performed at 37°C. Compartmentalized dye yielded a somewhat higher excitation ratio but was similarly $[Na^+]$-sensitive to the cytoplasm. Because of this, and because the volume of the compartmentalized dye represented a minor fraction of the total cellular volume, we determined $[Na^+]_i$ by averaging pixel intensities throughout the cell with subsequent conversion by calibrations. We converted intracellular SBFI fluorescence ratios to $[Na^+]_i$ by exposing cells to various extracellular $[Na^+]$ in the presence of 5 μM gramicidin in the standard medium, except that Cl^- was reduced to 60 mM (gluconate substitution), the $[Cl^-]_i$ in single parotid acinar cells (*7*), to prevent cell swelling. $[Na^+]$ in the bathing medium was altered by isosmotic replacement with K^+. The dissociation constant K_d for the dye was 22 mM. The data fitted reasonably well the equation $[Na^+]_i = K_d B (R - R_0)/(R_{max} - R)$, where R_0 and R_{max} are the measured ratios in the absence and in the presence of saturating (150 mM) intracellular $[Na^+]$, respectively, and B is the ratio of the emission intensities determined at 380-nm excitation for free and bound indicator. B was estimated to be 1.3 and R_{max}/R_0 to be 3.0. The upper limit for accurate $[Na^+]_i$ quantitation was ~80 to 100 mM.
13. The rapid cell shrinkage associated with the large-amplitude $[Ca^{2+}]_i$ spikes was not initially associated with a change in $[Na^+]_i$. A rise of $[Na^+]_i$ by ~20% would be expected on the basis of a 20% cell volume reduction. With average $[Na^+]_i$ ~9 mM, the expected rise in $[Na^+]_i$ would be ~1.8 mM, which is just at the level of resolution in our system.
14. Near saturation of the dye by $[Na^+]$ higher than ~100 mM limited our ability to resolve the $[Na^+]_i$ reached during some $[Na^+]_i$ transients associated with $[Ca^{2+}]_i$ oscillations. To compute the statistics, we assumed that $[Na^+]_i$ reached in these cells during such transients (nine out of 55 cells) was 100 mM. Similarly, during ouabain inhibition $[Na^+]_i$ usually rose to concentrations that were not resolvable with the dye.
15. M. Wong and J. K. Foskett, unpublished data.
16. In most cells, intracellular osmolarity is determined by the sum of the concentrations of Na^+, K^+, Cl^-, and impermeant anionic macromolecules (A^-). Because highly water-permeable cell membranes ensure that intracellular osmolarity equals that of the extracellular medium, and preservation of electrical neutrality dictates that $[Na^+]_i + [K^+]_i = [Cl^-]_i + [A^-]_i$, it follows that $[Na^+]_i + [K^+]_i$ contributes half of the cellular osmolarity. Our experiments were performed in isosmotic media; consequently, $[Na^+]_i + [K^+]_i$ always equals ~150 mM, regardless of the cell volume at different times in the oscillation cycle. Calculations of changes in intracellular Na^+ and K^+ contents, from $[Na^+]_i$ and $[K^+]_i$ and cell volume, indicate that neither Na^+ content, K^+ content, nor their sum, are constant during the oscillations. A detailed analysis of the changes in ion concentrations and contents during oscillations is in preparation.
17. Phospholipase C–mediated agonists, the Ca^{2+} ionophore ionomycin, and nystatin (to increase Na^+ entry) each greatly increases O_2 consumption in salivary acinar cells, which are entirely ouabain-sensitive [S. P. Soltoff *et al.*, in (*9*)].
18. J. K. Foskett, *Am. J. Physiol.* **255**, C566 (1988).

19. Supported by the Canadian Cystic Fibrosis Foundation (CCFF). M.M.Y.W. is a CCFF predoctoral fellow. J.K.F. is a CCFF scholar. We thank Q. Liu for technical assistance and S. Grinstein for comments.

20 June 1991; accepted 23 August 1991

GPI-Anchored Cell-Surface Molecules Complexed to Protein Tyrosine Kinases

IRENA STEFANOVÁ,*† VÁCLAV HOŘEJŠÍ, IGNACIO J. ANSOTEGUI, WALTER KNAPP, HANNES STOCKINGER

Binding of ligand or antibody to certain cell-surface proteins that are anchored to the membrane by glycophosphatidylinositol (GPI) can cause activation of leukocytes. However, it is not known how these molecules, which lack intracellular domains, can transduce signals. The GPI-linked human molecules CD59, CD55, CD48, CD24, and CD14 as well as the mouse molecules Thy-1 and Ly-6 were found to associate with protein tyrosine kinases, key regulators of cell activation and signal transduction. A protein tyrosine kinase associated with the GPI-linked proteins CD59, CD55, and CD48 in human T cells, and with Thy-1 in mouse T cells was identified as $p56^{lck}$, a protein tyrosine kinase related to Src. This interaction of GPI-linked molecules with protein tyrosine kinases suggests a potential mechanism of signal transduction in cells.

A VARIETY OF CELL-SURFACE PROTEINS are anchored in the membrane by glycophosphatidylinositol (GPI) (*1*). Some of these molecules are involved in cell adhesion or regulation of the complement system, but the physiological functions of most of them are unknown (*2*). Binding of natural ligands or antibodies to some GPI-linked proteins induces leukocyte activation (*3*). To explore the signal-transducing capacity of GPI-linked molecules, we studied transmembrane and intracellular molecules that are associated with them.

Many receptors have intrinsic or associated protein tyrosine kinase (PTK) activities that are required for signal transduction (*4*). Therefore, we analyzed phosphotransferase activity in immunoprecipitates of various GPI-anchored molecules. Protein kinase activity was co-precipitated with the GPI-linked human molecules CD59 (homologous restriction factor 20), CD55 (decay-accelerating factor), and CD48 from various types of cells, CD24 from B-chronic lymphoblastic leukemia (B-CLL) cells, CD14 from monocytes, and Thy-1 and Ly-6 from mouse cell lines (Fig. 1). In contrast, no protein kinase activity was detected in association with several other molecules that are anchored in the membrane of these cells

I. Štefanová, W. Knapp, H. Stockinger, Institute of Immunology--Vienna International Research Cooperation Center at SFI, University of Vienna, Brunner Strasse 59, A-1235 Vienna, Austria.
V. Hořejší, Institute of Molecular Genetics, Czechoslovak Academy of Sciences, 142 20 Prague 4, Vídeňská 1083, Czechoslovakia.
I. J. Ansotegui, Department of Immunology, Karolinska Institute, S-104 01 Stockholm, Sweden.

*To whom correspondence should be addressed.
†On leave from Institute of Molecular Genetics, Czechoslovak Academy of Sciences, 142 20 Prague 4, Vídeňská 1083, Czechoslovakia.